On the Role of Surface Fluxes and WISHE in Tropical Cyclone Intensification

FUQING ZHANG

Department of Meteorology, and Center for Advanced Data Assimilation and Predictability Techniques, The Pennsylvania State University, University Park, Pennsylvania, and Program in Atmospheres, Oceans, and Climate, Massachusetts Institute of Technology, Cambridge, Massachusetts

KERRY EMANUEL

Program in Atmospheres, Oceans, and Climate, Massachusetts Institute of Technology, Cambridge, Massachusetts

(Manuscript received 5 January 2016, in final form 24 February 2016)

ABSTRACT

The authors show that the feedback between surface wind and surface enthalpy flux is an important influence on tropical cyclone evolution, even though, as with at least some classical instability mechanisms, such a feedback is not strictly necessary. When the wind speed is artificially capped in idealized numerical experiments, storm development is slowed and storms achieve a smaller final intensity. When it is capped in simulations of an actual storm (Hurricane Edouard of 2014), the quality of the simulations is strongly compromised; for example, little development occurs when the wind speed is capped at 5 m s^{-1}, in contrast to the category-3 hurricane shown by observations and produced by the control experiment.

1. Introduction

By the early 1950s, several researchers had concluded that tropical cyclones are powered by enthalpy fluxes from the ocean (Riehl 1950; Kleinschmidt 1951). This was consistent with the observation that tropical cyclones only develop where there exists significant potential for heat fluxes from the sea and that these storms invariably decay over land even when moisture and instability are plentiful. But Charney and Eliassen (1964) argued that the initial intensification of tropical cyclones occurred through an organization of convection that they christened conditional instability of the second kind (CISK). Although they did not explicitly discuss the energetics of such a process, their formulation implied that the source of energy is the moist available potential energy of a conditionally unstable atmosphere. Emanuel (1986), echoing the earlier work by Riehl and Kleinschmidt, proposed instead that ''the intensification and maintenance of tropical cyclones depend *exclusively*[1] on self-induced heat transfer from the ocean,'' arguing that ambient conditional instability plays essentially no role, with energy supplied exclusively by surface enthalpy fluxes. A key adjective in this formulation is ''self-induced,'' the idea being that the winds associated with the tropical cyclones drive the surface enthalpy fluxes that power it—a process that has since been called ''wind-induced surface heat exchange'' (WISHE).

Thus, there are two areas of contention: 1) whether the development of tropical cyclones is powered by ambient conditional instability or by surface enthalpy fluxes local to the disturbance and 2) whether in the latter case the wind dependence of the surface fluxes is essential or incidental. Before continuing, it is worth noting a third possibility—namely, that the early stages of tropical cyclone development are powered or strongly influenced by interactions among radiation, clouds, and water vapor, similar to what happens in nonrotating self-aggregation of convection (e.g., Khairoutdinov and Emanuel 2013).

It is evident from the work of Montgomery et al. (2009, 2015), among others, that the wind dependence of surface fluxes is not necessary for the intensification

Corresponding author address: Professor Fuqing Zhang, Department of Meteorology, The Pennsylvania State University, 503 Walker Building, University Park, PA 16802.
E-mail: fzhang@psu.edu

DOI: 10.1175/JAS-D-16-0011.1

[1] Italics as in original.

of tropical cyclones. Our purpose here is merely to set this finding in the general context of stability theory and then to show that the wind dependence is quantitatively important and may make the difference between development and nondevelopment in real-world circumstances in which negative influences such as vertical wind shear are present. We proceed with a discussion of the role of feedbacks in stability.

2. Role of feedback in instability

Classical linear instabilities exhibit exponential growth owing to positive feedbacks among the variables. It is instructive to examine what happens if one of those variables is capped. As an illustration, we consider a pair of ordinary differential equations governing convection. These equations are developed in the appendix. Their nondimensional form is

$$\frac{dw}{dt} = B - w|w| \tag{1}$$

and

$$\frac{dB}{dt} = w, \tag{2}$$

where B and w represent nondimensional buoyancy and vertical velocity, respectively. The first equation expresses that the growth of vertical velocity is proportional to buoyancy and is retarded in proportion to the velocity squared. The second describes the growth of buoyancy as air ascends through unstable stratification. The Lagrangian equations are linearized by neglecting the last term in (1), and the linear solution exhibits exponential growth in time: $[B, w] \sim e^t$. We might describe this instability as resulting from a mutual feedback between vertical velocity, which increases the buoyancy, and buoyancy, which increases the vertical velocity. We might say that "convection is driven by buoyancy" and that "convective instability results from a feedback between vertical velocity and buoyancy."

Now suppose one artificially caps the buoyancy term that appears in (1):

$$\frac{dw}{dt} = \min(B, B_{\text{cap}}) - w^2, \tag{3}$$

where B_{cap} is a constant that serves to cap the magnitude of this term (assuming that we are thinking about the case where $B \geq 0$). If we now consider (2) and (3) and suppose, for the time being, that w is small enough to be neglected on the right-hand side of (3), we see that we get the same exponential growth for $B < B_{\text{cap}}$, but after that, the solution to (3) (including the last term) is

$$w' = \frac{\tanh(t') + w'_0}{1 + w'_0 \tanh(t')}, \tag{4}$$

where

$$w' \equiv \frac{w}{\sqrt{B_{\text{cap}}}}$$

and

$$t' \equiv 2\sqrt{B_{\text{cap}}}\,t,$$

where t is time measured from the time that the buoyancy first reaches its capping value and w'_0 is the value of the vertical velocity at that time.

It can be seen from (4) that once the capping buoyancy has been reached, the rate of growth begins to decrease and asymptotically approaches zero at large time, when the vertical velocity reaches a steady-state value given by $\sqrt{B_{\text{cap}}}$. Thus, capping the buoyancy affects both the rate of growth of the convection and the ultimate amplitude it achieves. Since this statement is true in the limit that $B_{\text{cap}} \to 0$, as long as B_{cap} is nonzero, we can state categorically that a feedback between vertical velocity and buoyancy is not necessary for the growth of convection, although we would continue to argue that convection is driven by buoyancy.

3. The case of tropical cyclones

Tropical cyclones represent an interesting departure from most classical instabilities, as it appears that the mechanisms responsible for their initiation and early development may be at least partially distinct from those that operate during their maturity. In particular, Rotunno and Emanuel (1987) and Emanuel (1989) demonstrated that the WISHE mechanism cannot destabilize the ordinary background state of the tropical atmosphere, and Emanuel (1989) showed that a mesoscale column of nearly saturated air must be attained before growth by WISHE can occur. Thus, it has been clear from the origins of WISHE theory that it cannot explain genesis and that some other process or processes must work to bring the system to such a state that WISHE could conceivably lead to further amplification. By this time, the system may be well past the stage at which linear theory could be considered valid. Mechanisms that have been proposed for the initiation and early intensification of tropical cyclones include various ways of organizing the release of ambient conditional instability, such as CISK (Charney and Eliassen 1964), merger of mesoscale vortices (e.g., Simpson et al. 1997;

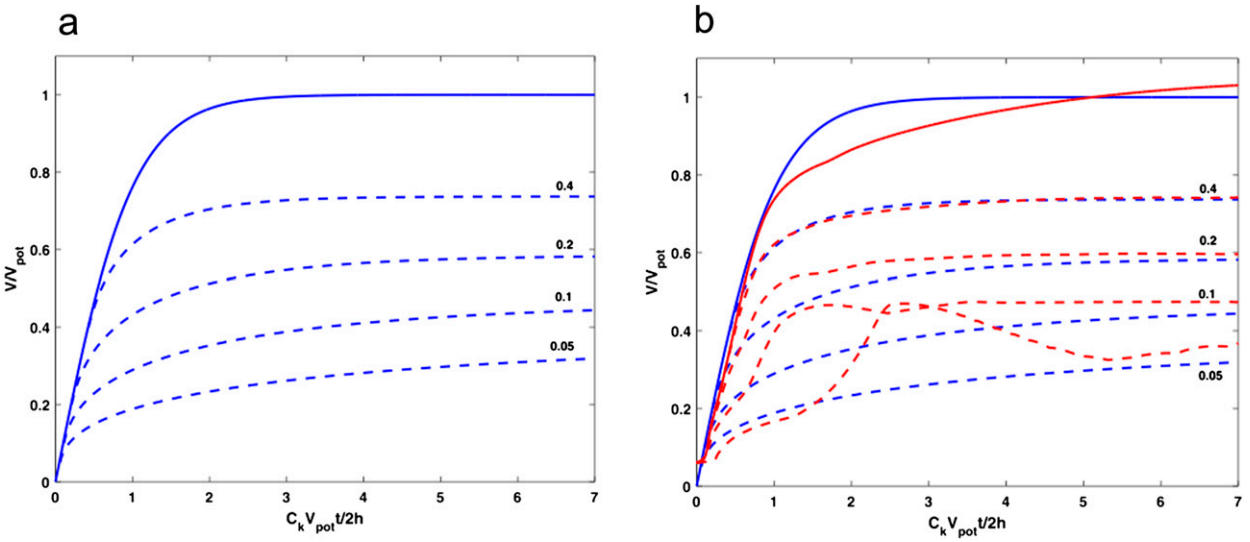

FIG. 1. (a) Approximate analytic solutions for the maximum gradient wind in tropical cyclones, given by (7) (solid) and (10) (dashed). In the latter case, solutions are plotted for the values of V_{cap}/V_{pot} indicated. Solutions are plotted for maximum wind scaled by potential intensity and time scaled by $2h/(C_k V_{pot})$. (b) These solutions are compared to numerical solutions of the simple model of Emanuel (2012) (red) for the same set of values of V_{cap}/V_{pot}. In the numerical simulations, the effects of variable outflow temperature are retained.

Montgomery et al. 2006), and merger of vortical hot towers (e.g., Van Sang et al. 2008) or, more broadly, the aggregation of convectively induced vorticity anomalies (e.g., Fang and Zhang 2011). In addition, linear destabilization of the background tropical atmosphere by interactions between radiation, clouds, and/or water vapor could also lead to genesis and amplification of tropical cyclones (e.g., Khairoutdinov and Emanuel 2013; Melhauser and Zhang 2014). Yet, to the best of the authors' knowledge, all mechanisms proposed for the ultimate amplification and maintenance of tropical cyclones rely on surface enthalpy fluxes, whether or not they are influenced by the cyclone's wind field. Here we explore what role, if any, the feedback of cyclone winds on surface fluxes plays in the intensification of the storm.

To make progress, we capitalize on the finding by Emanuel (1989, 2012) that once a mesoscale column of nearly saturated air is established, WISHE can begin to amplify the disturbance. We do not claim that WISHE cannot have any effect before this stage or that whatever leads to core saturation suddenly ceases at this time, but using this as a starting point we can examine analytically and numerically the subsequent evolution of axisymmetric TCs and the extent to which it is influenced by the WISHE feedback.

Emanuel (2012) showed that, beginning with a saturated core with a fully developed tropopause anticyclone,[2] the nonlinear evolution of the peak wind speed V in an idealized, balanced, axisymmetric tropical cyclone model is given approximately by [cf. (17) from that paper]

$$\frac{\partial V}{\partial t} \cong \frac{C_k}{2h}(V_{\max}^2 - V^2), \tag{5}$$

where C_k is the surface exchange coefficient for enthalpy (assumed constant), h is the boundary layer depth, and

$$V_{\max}^2 \equiv \frac{C_k}{C_D} F\left(\frac{C_k}{C_D}\right) \frac{T_s - T_t}{T_s}(k_0^* - k_e), \tag{6}$$

where k_0^* is the saturation enthalpy of the sea surface; k_e is the environmental boundary layer enthalpy; T_s and T_t are the sea surface and ambient tropopause temperatures, respectively; C_D is the surface drag coefficient (assumed constant); and $F(C_k/C_D)$ is a function of C_k/C_D [defined by (18) of Emanuel (2012)] that derives from an assumption of outflow-layer Richardson number criticality. There are quite a few approximations that lead to (5), including the neglect of dissipative heating and the pressure dependence of the surface saturation enthalpy. To simplify the subsequent development to the point where analytic solutions are possible, we also approximate $F(C_k/C_D)$ by unity. This is equivalent to neglecting the dependence of outflow temperature on radius. Note that we will later relax this approximation in comparing our analytic solution to numerical solutions.

The solution to (5) without placing any limitations on the wind speed used in the surface enthalpy flux is [cf. (19) of Emanuel (2012)]

[2] Note that this assumption, while necessary to obtain analytic solutions, is not well satisfied in more realistic simulations such as those presented in section 4.

TABLE 1. Description of 13 numerical experimental configurations.

Expt	Surface enthalpy exchange coefficient ($\times 10^{-3}$)	Capping wind speed ($m\,s^{-1}$) in surface enthalpy flux
1 (control)	1	—
2	0.5	5
3	0.5	10
4	0.5	20
5	1	5
6	1	10
7	1	20
8	1.5	5
9	1.5	10
10	1.5	20
11	2	5
12	2	10
13	2	20

$$V = V_{\max} \tanh\left(\frac{C_k V_{\max}}{2h} t\right). \tag{7}$$

We can cap the wind speed used to calculate the surface enthalpy flux by replacing C_k with $C_k V_{\text{cap}}/V$ in (5) and (6) beginning at the time that V exceeds V_{cap}, the capping velocity used to calculate the surface enthalpy flux. The resulting equation can be written

$$\frac{\partial V^3}{\partial t} \cong \frac{3C_k V_{\text{cap}}}{2h}(V_{\text{cap}} V_{\text{pot}}^2 - V^3), \tag{8}$$

where V_{pot} is the "classical" potential intensity, given by

$$V_{\text{pot}}^2 \equiv \frac{C_k}{C_D}\frac{T_s - T_t}{T_t}(k_0^* - k_e). \tag{9}$$

Note that (8) is very similar to the capped convection equation [see (3)] except that the last term is linear (in V^3). The solution to (8) that satisfies the condition that $V = V_{\text{cap}}$ at $t = t_0$ is

$$V^3 = V_{\text{cap}} V_{\text{pot}}^2 \left\{1 - \left[1 - \left(\frac{V_{\text{cap}}}{V_{\text{pot}}}\right)^2\right] e^{(-3C_k V_{\text{cap}}/2h)(t-t_0)}\right\}. \tag{10}$$

It is clear from this solution that capping the wind speed used in the surface enthalpy flux affects both the ultimate amplitude of the wind speed and the rate of intensification. In particular, the maximum wind speed is $V_{\text{cap}}^{1/3} V_{\text{pot}}^{2/3}$. The uncapped solution in (7) is compared to solutions to (10) for four values of the ratio $V_{\text{cap}}/V_{\text{pot}}$ in Fig. 1a. Clearly, the growth of the solutions is substantially slowed after the maximum wind speed reaches the capping velocity, and the ultimate amplitude is noticeably diminished.

Figure 1b compares these solutions to the numerical solution of the time-dependent model developed by Emanuel (2012), for the case in which dissipative heating and the pressure dependence of the surface saturation

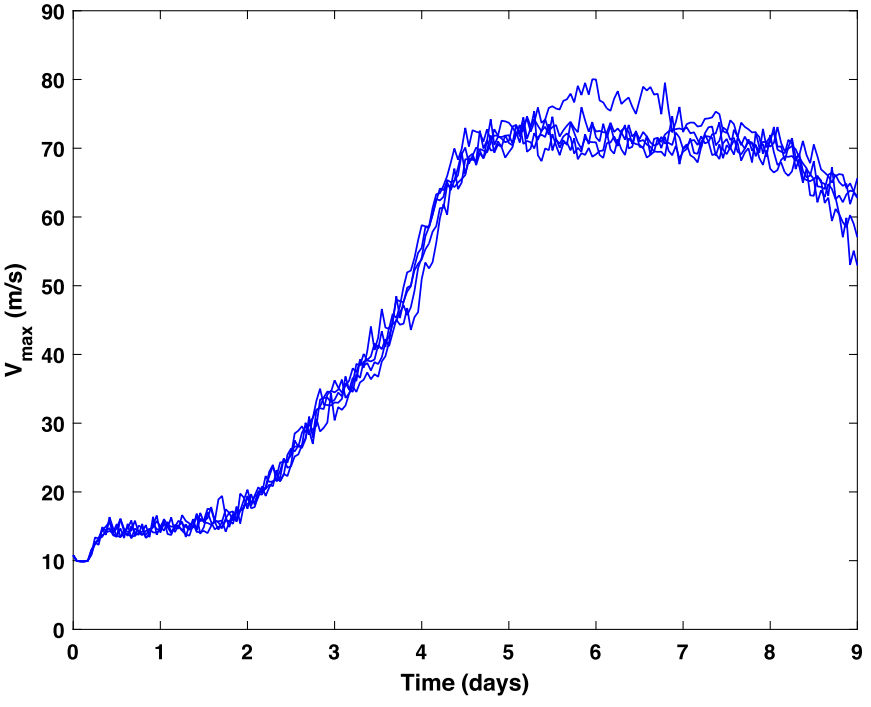

FIG. 2. Evolution over time of the peak wind speed of five ensemble members of numerical simulations corresponding to experiment 10 of Table 1.

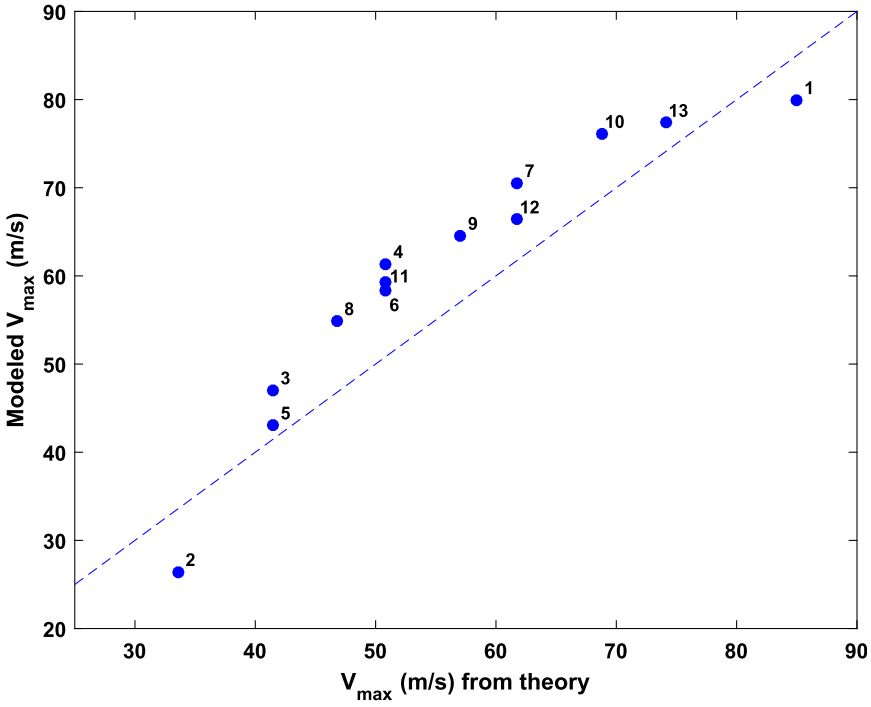

FIG. 3. Correspondence between theoretical maximum wind speed from Emanuel and Rotunno (2011; abscissa) and maximum wind speed achieved in the full-physics, three-dimensional numerical simulations (ordinate). The numbers correspond to the experimental configurations listed in Table 1.

enthalpy are neglected. But, unlike the analytic solutions given by (10), the full function dependence $F(C_k/C_D)$ is retained, so we expect the numerical solutions to depart from (10). Indeed, some of the simulations show large departures from the analytic solution during the intensification phase, though the steady-state intensities are not greatly different.

These simple models suggest that the wind dependence of the surface enthalpy flux (WISHE) strongly influences tropical cyclone intensification and ultimate intensity, even though it is not strictly necessary for intensification, at least under idealized circumstances. In the next section, we explore the role of WISHE in the development of tropical cyclones simulated by a nonhydrostatic, three-dimensional numerical model.

4. Role of WISHE in tropical cyclone development simulated by a three-dimensional nonhydrostatic model

a. *Model and experimental setup for idealized experiments*

The Advanced Research version of the Weather Research and Forecast (WRF) Model, version 3.1, with a 2-km grid spacing for the innermost nest is used. The model configuration for the control ensemble simulations is exactly the same as the "SH0" experiment in Zhang and Tao (2013). The ensemble is initialized with the same idealized modified Rankine vortex that has a maximum surface wind speed of 15 m s^{-1} at 135-km radius. The Dunion (2011) non–Saharan air layer mean hurricane season sounding is used for the environmental moisture and temperature profile while a constant sea surface temperature (27°C) and a constant Coriolis parameter equivalent to 20°N are used. As in Zhang and Tao (2013), within each ensemble, exactly the same environment conditions but different realizations of moisture perturbations with magnitude randomly selected from a uniform distribution of (−0.5, 0.5) g kg^{-1} are applied to all the model grid points below 950 hPa. We ran five ensemble members each in the configurations listed in Table 1. The control ensemble uses a fixed surface drag coefficient of 0.001 for all wind speed ranges, which is different from Zhang and Tao (2013), who used the tropical cyclone surface flux option 1 (isftcflx=1 in WRF namelist file) that caps the increase of drag coefficient when the surface wind speed reaches hurricane force (~33 m s^{-1}) following Donelan et al. (2004), as detailed in Green and Zhang (2013). A total of 12 other ensemble sensitivity experiments in which the surface enthalpy exchange coefficient and capping wind speeds were varied are listed in Table 1. In all the experiments listed, the

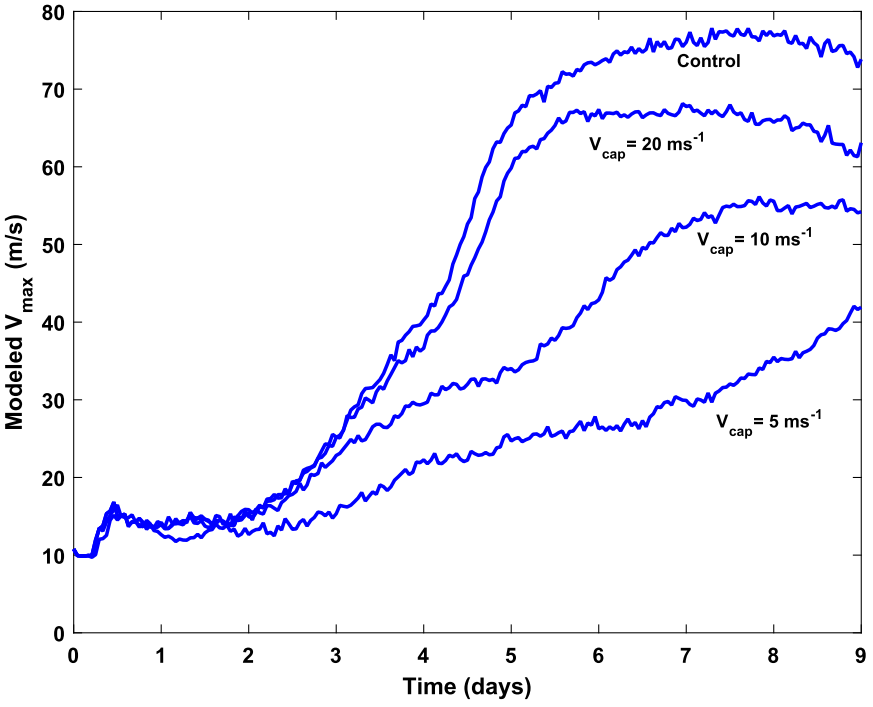

FIG. 4. Evolution over time of the ensemble mean of the four experiments for which $C_k = 1 \times 10^{-3}$. The curve labels are capping wind speeds.

surface exchange coefficients were fixed constants rather than being determined by the default surface layer scheme of the WRF Model.

b. *Results from idealized experiments*

Figure 2 shows the evolution over time of the peak wind speed of the five ensemble members of experiment 10 in which $C_k = 1.5 \times 10^{-3}$ and $V_{\text{cap}} = 20\,\text{m s}^{-1}$. There is not much divergence among the ensemble members, and the evolution is qualitatively similar to that of other numerical simulations under idealized environmental conditions. Note, however, that the peak rates of intensification occur roughly midway through the simulations rather than near the beginning as in the idealized theoretical models discussed in the previous section. This is probably because those idealized models begin from a state of core saturation, while the more realistic WRF simulations do not; thus, the latter must endure a gestation period while their cores approach saturation.

Peak winds vary between about 70 and $75\,\text{m s}^{-1}$, similar to the peak winds in the control ensemble of around $70\,\text{m s}^{-1}$.

To compare with the theoretical predictions of peak wind speed, we found the maximum over time of the peak wind speed of each ensemble member and averaged it over the five ensemble members to arrive at an estimate of the maximum wind speed for each experiment listed in Table 1. To calculate the theoretical maximum intensity for each value of the capping wind speed and enthalpy exchange coefficient, we began with (40) and (41) from Emanuel and Rotunno (2011) and substituted $C_k V_{\text{cap}}/V_m$ for C_k wherever it appears, iterating numerically to find the peak wind speed V_m. We note, however, that in addition to the usual assumptions of hydrostatic and gradient balance and axisymmetry underlying most potential intensity theories, dissipative heating has been neglected (as in the numerical simulations) as well as the pressure dependence of the surface saturation enthalpy, which is an approximation not made in the numerical model. As pressure falls in the storm core, saturation enthalpy increases, boosting storm intensity. Thus, we expect the theory to underpredict the intensity achieved by the numerical simulations, particularly at high intensity, when the pressure fall is particularly large. On the other hand, the theory neglects radial mixing while the numerical model includes radial mixing both by explicit three-dimensional eddies and by parameterized turbulence. By weakening the storm, radial mixing will work qualitatively in the opposite direction from the neglect of pressure dependence of surface saturation enthalpy in the theory.

Bearing in mind these caveats, Fig. 3 compares the maximum wind predicted by theory to that achieved in the numerical simulations. While not perfect, there is a good correspondence between the numerical simulations and the theory advanced by Emanuel and Rotunno (2011). In

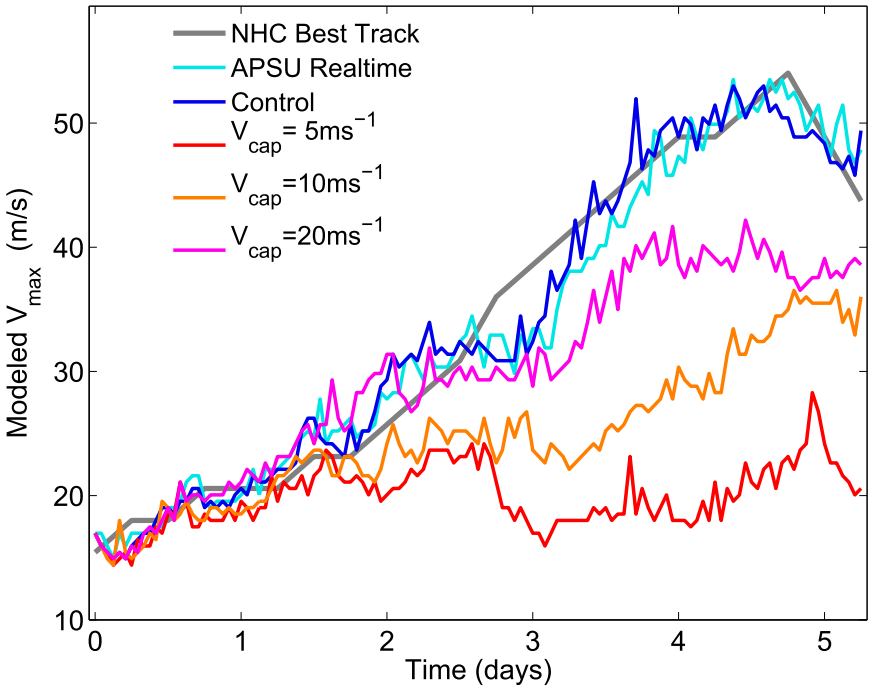

FIG. 5. Evolution over time of the peak wind in Hurricane Edouard (2014) from the National Hurricane Center's best-track data (gray), in the PSU experimental real-time forecast (cyan), in the control experiment (blue), and in experiments in which the wind used to calculate surface enthalpy fluxes is capped at 5 (red), 10 (orange), and 20 m s^{-1} (purple).

general, the theory underestimates the actual wind speed, and at least part of this may be owing to the fact that the actual wind exceeds the gradient wind to which the theory pertains (e.g., Smith and Montgomery 2008).

Figure 4 compares the time evolutions of the ensemble means of the four simulations for which $C_k = 1 \times 10^{-3}$. At least qualitatively, the rate of intensification of the capped experiments is smaller than that of the control, as predicted.

c. *A real-world case study: Hurricane Edouard (2014)*

We further performed similar sensitivity experiments as in the idealized simulations of Fig. 4 except using the real-world event of Hurricane Edouard (2014). The control simulation uses WRF, version 3.5.1, the same model configuration as The Pennsylvania State University (PSU) experimental real-time hurricane analysis and prediction system based on WRF and an ensemble Kalman filter (EnKF), described in Weng and Zhang (2016), except that the enthalpy exchange coefficient is fixed at 0.001 for all wind speed ranges. The control simulation is initialized with the PSU real-time WRF–EnKF mean analysis starting at 1200 UTC 11 September 2014 integrated for 126 h. The innermost domain grid spacing is 3 km with 298 × 298 horizontal grid points movable centered on the tropical cyclone center.

Figure 5 compares the evolution over time of the peak wind of Edouard from best-track data and the PSU experimental real-time forecast to that of the control simulation and three other experiments in which the wind speed that appears in the surface enthalpy flux relations has been capped. The control simulation with fixed enthalpy exchange coefficient produces a very similar intensity forecast to the PSU experimental real-time prediction ("APSU") that agrees well with the NHC best-track estimate with a category-3 peak intensity. Capping surface fluxes at decreasingly smaller surface wind speed results in much weaker storms to no storms developed at all. Clearly in at least some real-world cases in which the tropical cyclone is influenced by external factors—for example, vertical shear of the environmental wind—the WISHE feedback is quantitatively important and may make the difference between growth and decay. There will be no *Hurricane* Edouard in this case if the surface enthalpy flux is capped at the wind speed of 5 m s^{-1}.

5. Summary

The WISHE feedback is no more essential for tropical cyclone intensification than any feedback is in any classical instability once a reasonable amplitude is achieved. But, as shown here, it nevertheless strongly

influences both the rate of development and the ultimate intensity achieved by storms in idealized environments. When the wind speed is capped in the surface enthalpy flux, the steady intensity is given by $V_{\rm cap}^{1/3}V_{\rm pot}^{2/3}$. Under less favorable conditions, such as when environmental wind shear is present, WISHE may make the difference between development and nondevelopment.

As a semantical point, the term ''WISHE'' has come to be used to distinguish theories relying on surface enthalpy fluxes to power tropical cyclones from other theories, such as CISK, in which ambient conditional instability serves as the energy source. We note here that the original paper defining CISK (Charney and Eliassen 1964) also defined tropical cyclone intensification in terms of a feedback: ''The cumulus- and cyclone-scale motions are thus to be regarded as cooperating rather than as competing—the clouds supplying latent heat energy to the cyclone, and the cyclone supplying the fuel, in the form of moisture, to the clouds.'' While it might be better to distinguish tropical cyclone intensification mechanisms by their energy sources, the CISK-versus-WISHE dichotomy has gained some currency (e.g., Craig and Gray 1996) and for this reason may remain the preferred terminology.

Acknowledgments. This study is performed primarily during the lead author's sabbatical visit at MIT during fall 2015 sponsored by the Houghton Lecturer Fund as well as the NSF Grant AGS 1305798 and ONR Grant N000140910526. The second author gratefully acknowledges support from ONR through Grant N000141410062. The authors thank Dandan Tao, Yonghui Weng, and Ben Green for their help on the WRF experiments. We also benefited from comments from three anonymous reviewers on an earlier version of the manuscript as well as from discussions on this subject with Dan Chavas, Mike Montgomery, Heather Archambault, Rich Rotunno, and others. Computing was conducted at the Texas Advanced Computing Center.

APPENDIX

Simplified Convection Equations

Here we develop simple Lagrangian equations governing the adiabatic ascent of a buoyant, nonentraining thermal that does, however, experience aerodynamic drag. We begin with the vertical equation of motion in which the pressure gradient term has been linearized about a hydrostatic state [cf. chapter 1 of Emanuel (1994)]:

$$\frac{dw}{dt} = g\frac{\theta'}{\overline{\theta}} - \frac{1}{\overline{\rho}}\frac{\partial p'}{\partial z}, \tag{A1}$$

where w is the vertical velocity; g is the acceleration of gravity; θ' and $\overline{\theta}$ are the perturbation and resting-state potential temperatures, respectively; $\overline{\rho}$ is the resting state density; and p' is the perturbation (nonhydrostatic) pressure.

We assume an atmosphere in which the potential temperature decreases linearly with altitude, so that a sample displaced upward by an amount δz experiences a buoyancy given by

$$B' \equiv g\frac{\theta'}{\overline{\theta}} = N^2\delta z, \tag{A2}$$

where

$$N^2 \equiv \frac{-g}{\overline{\theta}}\frac{d\overline{\theta}}{dz}.$$

We model the second term in (A1) as an aerodynamic drag, which depends on the aspect ratio of the thermal and its velocity according to

$$\frac{1}{\overline{\rho}}\frac{\partial p'}{\partial z} = \alpha|w|w, \tag{A3}$$

where α is a coefficient with dimensions of inverse length. Inserting (A3) into (A1) gives

$$\frac{dw}{dt} = B' - \alpha|w|w. \tag{A4}$$

Finally, an alternative to (A2) may be formulated by differentiating it in time:

$$\frac{dB}{dt} = N^2 w. \tag{A5}$$

To arrive at the final dimensionless forms of (A4) and (A5), given by (1) and (2) in the main text, we normalize the dependent and independent variables as follows:

$$t \to N^{-1}t,$$
$$B' \to N^2\alpha^{-1}B,$$
$$w \to N\alpha^{-1}w.$$

REFERENCES

Charney, J. G., and A. Eliassen, 1964: On the growth of the hurricane depression. *J. Atmos. Sci.*, **21**, 68–75, doi:10.1175/1520-0469(1964)021<0068:OTGOTH>2.0.CO;2.

Craig, G. C., and S. L. Gray, 1996: CISK or WISHE as the mechanism for tropical cyclone intensification. *J. Atmos.*

Sci., **53**, 3528–3540, doi:10.1175/1520-0469(1996)053<3528:COWATM>2.0.CO;2.

Donelan, M. A., B. K. Haus, N. Reul, W. J. Plant, M. Stiassnie, H. C. Graber, O. B. Brown, and E. S. Saltzman, 2004: On the limiting aerodynamic roughness of the ocean in very strong winds. *Geophys. Res. Lett.*, **31**, L18306, doi:10.1029/2004GL019460.

Dunion, J. P., 2011: Rewriting the climatology of the tropical North Atlantic and Caribbean Sea atmosphere. *J. Climate*, **24**, 893–908, doi:10.1175/2010JCLI3496.1.

Emanuel, K. A., 1986: An air–sea interaction theory for tropical cyclones. Part I: Steady-state maintenance. *J. Atmos. Sci.*, **43**, 585–605, doi:10.1175/1520-0469(1986)043<0585:AASITF>2.0.CO;2.

——, 1989: The finite-amplitude nature of tropical cyclogenesis. *J. Atmos. Sci.*, **46**, 3431–3456, doi:10.1175/1520-0469(1989)046<3431:TFANOT>2.0.CO;2.

——, 1994: *Atmospheric Convection*. Oxford University Press, 580 pp.

——, 2012: Self-stratification of tropical cyclone outflow. Part II: Implications for storm intensification. *J. Atmos. Sci.*, **69**, 988–996, doi:10.1175/JAS-D-11-0177.1.

——, and R. Rotunno, 2011: Self-stratification of tropical cyclone outflow. Part I: Implications for storm structure. *J. Atmos. Sci.*, **68**, 2236–2249, doi:10.1175/JAS-D-10-05024.1.

Fang, J., and F. Zhang, 2011: Evolution of multiscale vortices in the development of Hurricane Dolly (2008). *J. Atmos. Sci.*, **68**, 103–122, doi:10.1175/2010JAS3522.1.

Green, B. W., and F. Zhang, 2013: Impacts of air–sea flux parameterizations on the intensity and structure of tropical cyclones. *Mon. Wea. Rev.*, **141**, 2308–2324, doi:10.1175/MWR-D-12-00274.1.

Khairoutdinov, M., and K. Emanuel, 2013: Rotating radiative-convective equilibrium simulated by a cloud-resolving model. *J. Adv. Model. Earth Syst.*, **5**, 816–825, doi:10.1002/2013MS000253.

Kleinschmidt, E., Jr., 1951: Grundlagen einer theorie der tropischen zyklonen. *Arch. Meteor. Geophys. Bioklimatol.*, **4A**, 53–72, doi:10.1007/BF02246793.

Melhauser, C., and F. Zhang, 2014: Diurnal radiation cycle impact on the pregenesis environment of Hurricane Karl (2010). *J. Atmos. Sci.*, **71**, 1241–1259, doi:10.1175/JAS-D-13-0116.1.

Montgomery, M. T., M. E. Nicholls, T. A. Cram, and A. B. Saunders, 2006: Vortical hot tower route to tropical cyclogenesis. *J. Atmos. Sci.*, **63**, 355–386, doi:10.1175/JAS3604.1.

——, N. V. Sang, R. K. Smith, and J. Persing, 2009: Do tropical cyclones intensify by WISHE? *Quart. J. Roy. Meteor. Soc.*, **135**, 1697–1714, doi:10.1002/qj.459.

——, J. Persing, and R. K. Smith, 2015: Putting to rest WISHE-ful misconceptions for tropical cyclone intensification. *J. Adv. Model. Earth Syst.*, **7**, 92–109, doi:10.1002/2014MS000362.

Riehl, H., 1950: A model for hurricane formation. *J. Appl. Phys.*, **21**, 917–925, doi:10.1063/1.1699784.

Rotunno, R., and K. A. Emanuel, 1987: An air–sea interaction theory for tropical cyclones. Part II: Evolutionary study using a nonhydrostatic axisymmetric numerical model. *J. Atmos. Sci.*, **44**, 542–561, doi:10.1175/1520-0469(1987)044<0542:AAITFT>2.0.CO;2.

Simpson, J., E. A. Ritchie, G. Holland, J. Halverson, and S. Stewart, 1997: Mesoscale interactions in tropical cyclone genesis. *Mon. Wea. Rev.*, **125**, 2643–2661, doi:10.1175/1520-0493(1997)125<2643:MIITCG>2.0.CO;2.

Smith, R. K., and M. T. Montgomery, 2008: Balanced boundary layers used in hurricane models. *Quart. J. Roy. Meteor. Soc.*, **134**, 1385–1395, doi:10.1002/qj.296.

Van Sang, N., R. K. Smith, and M. T. Montgomery, 2008: Tropical-cyclone intensification and predictability in three dimensions. *Quart. J. Roy. Meteor. Soc.*, **134**, 563–582, doi:10.1002/qj.235.

Weng, Y., and F. Zhang, 2016: Advances in convection-permitting tropical cyclone analysis and prediction through EnKF assimilation of reconnaissance aircraft observations. *J. Meteor. Soc. Japan*, doi:10.2151/jmsj.2016-018, in press.

Zhang, F., and D. Tao, 2013: Effects of vertical wind shear on the predictability of tropical cyclones. *J. Atmos. Sci.*, **70**, 975–983, doi:10.1175/JAS-D-12-0133.1.